ISSN: 0975-833X

Available online at http://www.journalcra.com

International Journal of Current Research
Vol. 8, Issue, 12, pp.43542-43547, December, 2016

INTERNATIONAL JOURNAL OF CURRENT RESEARCH

RESEARCH ARTICLE

AN AUTOMATIC PROBABILISTIC FRAMEWORK FOR BRAIN TUMOUR DETECTION USING MR IMAGES

***,[1]Nageswara Reddy, P., [2]Mohan Rao, C. P. V. N. J. and [3]Ch.Satyanarayana**

[1]Research Scholar, Jawaharlal Nehru Technological University, Kakinada
[2]Professor and Principal, Avanthi Institute of Engineering & Technology
[3]Professor, Department of Computer Science and Engineering, JNTU Kakinada

ARTICLE INFO

Article History:
Received 23rd September, 2016
Received in revised form
10th October, 2016
Accepted 29th November, 2016
Published online 30th December, 2016

Key words:

Brain MR Images, T1, T2, T1C, Flair, EM-GM Method, Multilateral Filter, Disorder Detection.

ABSTRACT

Improvement of automated frameworks for detection of brain tumour is the real need of the clinical enhancement. A Moderate numbers of methods are introduced to analyse the biological symptoms and produce the report to be recognized by the trained professions. Conversely, the final analysis is prone to errors due because of human interpretations. Also the computer aided reports leave huge scope for multiple further diagnoses. Thus the need of a novel algorithm for predictive analysis of diseases for brain disorder is much expected. This paper presents a fully reliable brain disease detection mechanism based on an enhancement in accuracy of multilateral filter and EM-GM method. The multilateral filter enhances the image edges for better segmentation using signal amplitude moderation of the pixel. The final outcome of this paper produces the brain regions detected with anomalies and possible diseases, thus the number of possible further medical investigations are reduces.

Copyright©2016, Nageswara Reddy et al. *This is an open access article distributed under the Creative Commons Attribution License, which permits unrestricted use, distribution, and reproduction in any medium, provided the original work is properly cited.*

Citation: Nageswara Reddy, P., Mohan Rao, C. P. V. N. J. and Ch.Satyanarayana, 2016. "An automatic probabilistic framework for brain tumour detection using MR images", *International Journal of Current Research,* 8, (12), 43542-43547.

INTRODUCTION

The Detection of brain tumours are the key area of focus for many researchers. The process of detection is manual and prune to human errors. Thus, the researchers are bounds to carry out multiple autonomous framework based researches. Gliomas are the highly in-focus and malignant type of tumours originated from the glial cells in the brain. Due to the malignant type, they grow fast in the surrounding cells and turns into high grade type of glioma. After the detection of these types of tumour, the life span of the patient is eventually reduced to two to three years and prerequisites a gastric pre and post neurosurgical procedure. Nonetheless, the detection delay can reduce the life span further. Due to the criticalness of the type, patients need to undergo for extraordinary frequency of diagnosis and the client results in gigantic amount of datasets. Processing those datasets manually is extremely effort consuming. The collected dataset are eventually entailing with quantitative information and can be best captured in MRI methods.The MR Image method reproduces the tumour information in 3D and 4D structures with the quantified boundaries. Nevertheless, the process of representation and detection remains a difficult process as the glioma tumours preserve to grow (Menze *et al*., 2014). Thus the predictive models of segmentation perform better in these situations. The framework, cited and proposed by many researchers, also includes a normalization phase, where the MR Image is being enhanced. Also the image modality can differ as MRI – T2 or MRI – FLAIR based on the segmentation algorithms used. This is proven that, various segmentation algorithms perform better on different types of MR Images. The recent researches also fail to achieve the unsurpassed accuracy (Bauer *et al*., 2013). Henceforth the rest of the paper is furnished with the focus to exhibit the improvement in accuracy of disorder detection for T1, T2, T1C and FLAIR type MR Images.

****Corresponding author: Nageswara Reddy,***
Research Scholar, Jawaharlal Nehru Technological University, Kakinada

Generic process of gliomas tumour types from MR images

The following are the steps for detecting brain tumour in human using MRI scan.

A. Image Acquisition

In MRI scan we get images of brain and these scanned images will display in two dimensional matrices along with their pixels as its elements. Matrices will be dependent on size of the matrix and its field of view. The scanned images will be

stored in the file and will be displayed as a grey scale image which ranges from 0 to 255. Where 0 shows the total black colour and 255 shows the entire white colour in which ranges vary intensity between black and white

B. Pre-Processing Stage

In this stage noise reduction and enhancement techniques are implemented for obtaining the best result of an image. These results in more prominent edges and a sharpened image is obtained, noise will be reduced thus reducing the blurring effect from the image. In addition to this image segmentation (edge detection method) is applied which helps in detecting the edges of image for finding the exact location of the tumour.

1) Text Removal: In this stage all unwanted text-noise will be removed. As the MRI scanned image may contain some text in image
2) Noise Removal: In this stage different types Low pass filters are used to remove the noise from the images. Filters are used to remove salt and pepper noise from the image. This filter pixel's value is replaced with its neighbourhood values.
3) Image Sharpening: After removing noise from the image the image is sharpened by using different high pass filters like Gaussian high pass filter that are widely used for sharpening the edges, which helps in detecting the boundaries of the tumour.

C. Skull Stripping

Skull striping is an important in medical image. It is done only to brain part, since it has to eliminate non brain tissues like extra cerebral tissues, fat, skin etc., it can be done by several techniques.

D. Processing Stage

In this stage segmentation of the image is done based on the division of the image of similar attributes into regions. These regions are grouped depending upon the similarity that helps in extracting the important features which information can be easily perceived.

E. Post-Processing Stage

In this processing stage segmentation of are done using different types of techniques or methods using algorithms which help for detecting accurate and effective location of tumour from brain. Some of the techniques or methods for segmentation are: watershed Segmentation, Threshold Segmentation, K-Means, Fuzzy C-Means… etc.

F. Morphological Operators

After conversion of image to binary format some morphological operations are performed to separate tumour part from the image. Only tumour part is visible in white in colour. The tumour portion contains highest intensity than other any regions of the image. This paper describes the applicability and improvement on tumour detection using EM-GM method. Thus the next section describes the functional parameters of EM-GM method.

EM – GM Method

In this section, the work explains the original EM – GM method and evaluates the applicability for image segmentation. Considering x is set of n independent sample of a mixture of multivalued distribution with dimension d.

$$x = (x_1, x_2, x_3, ...x_n) \tag{1}$$

and

Z is the connecting set of variable determines the component from which the result should be collected.

$$z = (z_1, z_2, z_3, ...z_n) \tag{2}$$

Thus,

$$X_i \mid (Z_i = 1) \square \mathrm{N}_d(\mu_1, \Sigma_1) \tag{3}$$

and

$$X_i \mid (Z_i = 2) \square \mathrm{N}_d(\mu_2, \Sigma_2) \tag{4}$$

Where

$$P(Z_i = 1) = \tau_1 \tag{5}$$

and

$$P(Z_i = 2) = \tau_2 = 1 - \tau_1 \tag{6}$$

Also the mixing value is calculated,

$$\theta = (\tau, \mu_1, \mu_2, \Sigma_1, \Sigma_2) \tag{7}$$

Thus the likelihood function can be represented as,

$$L(\theta; \mathbf{x}) = \prod_{i=1}^{n} \sum_{j=1}^{2} \tau_j \, f(\mathbf{x}_i; \boldsymbol{\mu}_j, \Sigma_j), \tag{8}$$

Hence, the complete likelihood function is represented as,

$$L(\theta; \mathbf{x}, \mathbf{z}) = p(\mathbf{x}, \mathbf{z} \mid \theta) = \prod_{i=1}^{n} \sum_{j=1}^{2} \mathrm{I}(z_i = j) \, f(\mathbf{x}_i; \boldsymbol{\mu}_j, \Sigma_j) \tau_j \tag{9}$$

Henceforth, in the next section this work proposed the automatic probabilistic framework for tumour detection.

Proposed Framework

The major focus of this work is to increase the accuracy of the detection of brain anomalies for MR Images. The magnetic resonance techniques for generating the visual representation of brain images result in two different types of images as T1 image and T2 image. The studies demonstrate the accuracy of T1 images is higher for detecting the anomalies. Hence in this work we focus on T1 images to carry out the proposed method. The core framework is been demonstrated here (Fig. 1).

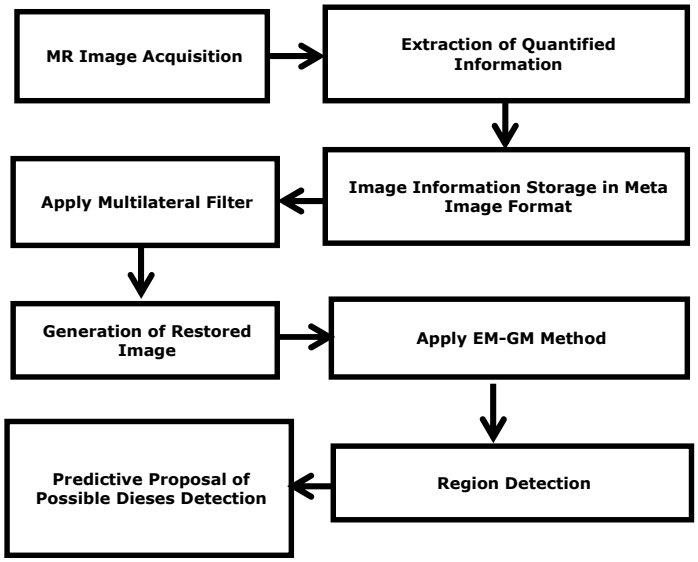

Fig.1. Proposed framework for Brain Anomaly Detection

A. Novel Multilateral Filter

The Proposed multilateral filter is based on the existing bilateral filter for improving the input image variance and standard deviation (Stille*et al*., 1965; Subbanna*et al*., 2013).

The bilateral filter explained as

$$\overline{IMG}(Co_1) = \frac{1}{N(Co_1)} \sum_{Co_1 \in Px} IMG(Co_2).g(Co_1, Co_2).P(IMG(Co_2), IMG(Co_1)) \quad (10)$$

Where,

IMG, denotes the original image

$\overline{IMG}$, denotes the filtered and noise removed image

Co_1 and Co_2, denotes the spatial coordinates of the image

Px, denotes the collection of pixels around the noise

$N(Co_1)$, denotes the normalization constant for each pixel to restrict the value after normalization within geometric and photonic range denoted by Px

And g and p, denotes the geometric and photometric similarities of the image

Hence the enhancement of the image is proposed to regularize the local signal amplitude of every pixel value:

$$\overline{IMG}(Co_1) = \frac{1}{N(Co_1)} \sum_{Co_1 \in Px} IMG(Co_2).\theta(Co_1, Co_2, t) \quad (11)$$

As,

$$\theta(Co_1, Co_2, t) = (1 - a(Co_1)).g(Co_1, Co_2) + a(Co_1).g(Co_1, Co_2).P(IMG(Co_1), IMG(Co_2)).\sum_{i=1}^{D-1} d_i(Co_1, Co_2) \quad (12)$$

Where,

$a(Co_1)$, denotes the regularized local signal amplitude of the pixel

di, denotes the image dimensions for during noise removal

B. Enhanced Expectation Maximization and Gaussian Mixture

The existing Gaussian mixture method (Gooya*et al*., 2011; Weizman,2012; Avants*et al*., 2011) is applied for each pixel of the normalized image. After application of Gaussian mixture method, the expectation maximization needs to be applied. Thereafter, the Gaussian parameters are to be mapped into the score point and finally, the likelihood to be calculated to converge. Based on the region marks, this technique will predict the possible diseases (Table – 1)(Achanta*et al*.,2012; Hameeteman,2011; Ahmed*et al*., 2015). The predictions of diseases are demonstrated in results and discussion section of this paper.

Multilateral Filter Outcomes

The improvement in the input images are been recorded (Table – 2 to 5) and the improvement in variance and standard deviation is been observed. The improvements are visualized in this section (Fig. 2 to 5).

Table 1. Brain Anomalous Area and Prediction of Diseases

Brain Region	Predictable Diseases
Amygdala	Memory Loss, Anxiety, Phobia, Post – Traumatic Disorder
Prefrontal Cortex	Stress
Anterior Cingulate Cortex	ADHD, Schizophrenia, Depression
Hippocampus	Mood Disorder

Table 2. Improvement in the Input Data by Multilateral Filter – FLAIR

Image DatasetIn MHA	Actual Image Variance	Filtered Image Variance	Improvement	Actual Image Std. Deviation	Filtered Image Std. Deviation	Improvement
Dataset – 1	5060902.713	4915045.117	0.02882	69.797568	69.568505	0.003282
Dataset – 2	9554696.161	16036161.27	0.678354	77.144764	88.461004	0.146688
Dataset – 3	8616966.903	9325425.899	0.082217	73.134012	74.266098	0.01548
Dataset – 4	2898009.131	5441952.068	0.877824	58.438954	68.754658	0.176521
Dataset – 5	3297844.713	3310126.799	0.003724	60.892958	61.294396	0.006593
Dataset – 6	7956455.468	9209704.089	0.157513	61.032613	63.335792	0.037737
Dataset – 7	4355136.222	4923593.077	0.130526	68.444576	70.463172	0.029492
Dataset – 8	21368886.14	18066531.68	0.15454	63.106152	60.306925	0.044357
Dataset – 9	7298752.498	8231411.34	0.127783	71.921236	73.941303	0.028087
Dataset – 10	2239552.24	8164522.795	2.645605	60.061124	84.239216	0.402558

Table 3. Improvement in the Input Data by Multilateral Filter – T1

Image Dataset In MHA	Actual Image Variance	Filtered Image Variance	Improvement	Actual Image Std. Deviation	Filtered Image Std. Deviation	Improvement
Dataset – 1	4426745.687	19162216.05	3.328737	72.648616	104.887534	0.443765
Dataset – 2	8406091.46	26021378.86	2.095538	74.846144	99.801705	0.333425
Dataset – 3	16958827.91	19501273.64	0.149919	100.156664	103.583045	0.03421
Dataset – 4	17772628.04	19802241.38	0.114199	99.038213	102.016712	0.030074
Dataset – 5	13768559.75	14906214.22	0.082627	93.611389	95.94429	0.024921
Dataset – 6	22898252.69	24819950.25	0.083923	93.447251	95.434675	0.021268
Dataset – 7	22003154	24379743.81	0.108011	104.394753	106.962605	0.024598
Dataset – 8	15379577.02	16119083.29	0.048084	103.211526	104.673618	0.014166
Dataset – 9	9672979.152	11018602.43	0.139112	78.361981	81.946585	0.045744
Dataset – 10	9672979.152	11018602.43	0.139112	78.361981	81.946585	0.045744

Table 4. Improvement in the Input Data by Multilateral Filter – T2

Image Dataset In MHA	Actual Image Variance	Filtered Image Variance	Improvement	Actual Image Std. Deviation	Filtered Image Std. Deviation	Improvement
Dataset – 1	2893554.644	3752181.075	0.296738	60.258618	64.599329	0.072035
Dataset – 2	2406414.584	3177258.438	0.320329	50.748587	56.46155	0.112574
Dataset – 3	4859893.989	4779595.617	0.016523	66.462106	66.070983	0.005885
Dataset – 4	1722850.314	2062650.347	0.197231	47.485555	49.923533	0.051341
Dataset – 5	5053719.403	8311452.955	0.644621	63.456567	71.954974	0.133925
Dataset – 6	5053719.403	8311452.955	0.644621	63.456567	71.954974	0.133925
Dataset – 7	6116058.465	6181313.026	0.010669	56.694385	56.933726	0.004222
Dataset – 8	1655927.918	1632738.103	0.014004	50.417798	50.442167	0.000483
Dataset – 9	4688216.164	4697257.513	0.001929	68.233328	68.089125	0.002113
Dataset – 10	3213676.027	3928247.099	0.222353	61.218723	65.484408	0.069679

Table 5. Improvement in the Input Data by Multilateral Filter – T1C

Image Dataset In MHA	Actual Image Variance	Filtered Image Variance	Improvement	Actual Image Std. Deviation	Filtered Image Std. Deviation	Improvement
Dataset – 1	7293520.405	17192522.9	1.357232	80.733374	100.264884	0.241926
Dataset – 2	1829464.97	10392524.45	4.680636	51.132055	79.382207	0.552494
Dataset – 3	752554.5295	8586590.521	10.409925	43.737097	81.375867	0.860569
Dataset – 4	1008211.942	6543428.922	5.490132	47.294959	76.133189	0.609753
Dataset – 5	1823443.794	5016480.102	1.751102	54.81342	71.403739	0.302669
Dataset – 6	3550669.136	9953151.433	1.803176	58.35015	75.674243	0.296899
Dataset – 7	596971.6746	4443766.514	6.443848	45.598477	76.271296	0.672672
Dataset – 8	596971.6746	4443766.514	6.443848	45.598477	76.271296	0.672672
Dataset – 9	1948743.064	3492151.849	0.792002	52.0609	60.615936	0.164327
Dataset – 10	1901077.531	7470530.45	2.92963	59.159467	84.129712	0.422084

Table 6. Accuracy Analysis over Expectation Maximization – Gaussian Mixture Method – FLAIR

Image DatasetIn MHA format	EM – GM	Novel Unification Technique	Improvement (%)
Dataset – 1	97.78	99.01	1.26
Dataset – 2	98.11	99.11	1.02
Dataset – 3	97.02	98.02	1.03
Dataset – 4	93.71	94.71	1.07
Dataset – 5	95.87	96.87	1.04
Dataset – 6	94.3	95.3	1.06
Dataset – 7	92.48	93.48	1.08
Dataset – 8	95.1	96.1	1.05
Dataset – 9	89.28	90.28	1.12
Dataset – 10	98.08	99.08	1.02

Table 7. Accuracy Analysis over Expectation Maximization – Gaussian Mixture Method – T1

Image DatasetIn MHA format	EM – GM	Novel Unification Technique	Improvement (%)
Dataset – 1	96.97	99.13	2.23
Dataset – 2	98.12	99.12	1.02
Dataset – 3	91.53	92.53	1.09
Dataset – 4	91.67	92.67	1.09
Dataset – 5	95.63	96.63	1.05
Dataset – 6	93.04	94.04	1.07
Dataset – 7	94.25	95.25	1.06
Dataset – 8	92.03	93.03	1.09
Dataset – 9	85.43	86.43	1.17
Dataset – 10	97.54	98.54	1.03

RESULTS AND DISCUSSION

The optimal unification framework is been applied to FLAIR, T1, T2 and T1C image formats alongside with the EM-GM (Table – 6 to 9) techniques and a relative improvement in the result is observed. The improvements are visualized here (Fig. 6 to 9)

Hence this work shows the improvement of accuracy for all the tested datasets for 10 Datasets' dataset. The work also successfully predicts the diseases based on the anomalies detected on the brain regions. The outcomes of the predictive analysis is also demonstrated (Fig. 10) (Table – 10). This outcome makes the work unique in nature and reduced the span of further investigations.

Table 8. Accuracy Analysis over Expectation Maximization – Gaussian Mixture Method – T2

Image DatasetIn MHA format	EM – GM	Novel Unification Technique	Improvement (%)
Dataset – 1	95.99	97.03	1.08
Dataset – 2	98.29	99.29	1.02
Dataset – 3	91.64	92.64	1.09
Dataset – 4	91.86	92.86	1.09
Dataset – 5	95.36	96.36	1.05
Dataset – 6	92.87	93.87	1.08
Dataset – 7	92.18	93.18	1.08
Dataset – 8	91.57	92.57	1.09
Dataset – 9	85.5	86.5	1.17
Dataset – 10	97.46	98.46	1.03

Table 9. Accuracy Analysis over Expectation Maximization – Gaussian Mixture Method – T1C

Image DatasetIn MHA format	EM – GM	Novel Unification Technique	Improvement (%)
Dataset – 1	95.86	99.09	3.37
Dataset – 2	98.29	99.29	1.02
Dataset – 3	91.75	92.75	1.09
Dataset – 4	91.99	92.99	1.09
Dataset – 5	95.61	96.61	1.05
Dataset – 6	93.27	94.27	1.07
Dataset – 7	93.15	94.15	1.07
Dataset – 8	91.62	92.62	1.09
Dataset – 9	85.85	86.85	1.16
Dataset – 10	97.86	98.86	1.02

Table 10. Region Based Disease Prediction Results

Image DatasetIn MHA format	Regions Detected	Predicted Diseases
Dataset – 1	Hippocampus – Right	Mood Disorder
Dataset – 2	Anterior Cingulate Cortex	ADHD, Schizophrenia, Depression
Dataset – 3	Prefrontal Cortex and Amygdala	Stress, Memory Loss, Anxiety, Phobia, Post – Traumatic Disorder
Dataset – 4	Anterior Cingulate Cortex	ADHD, Schizophrenia, Depression
Dataset – 5	Hippocampus – Left	Mood Disorder

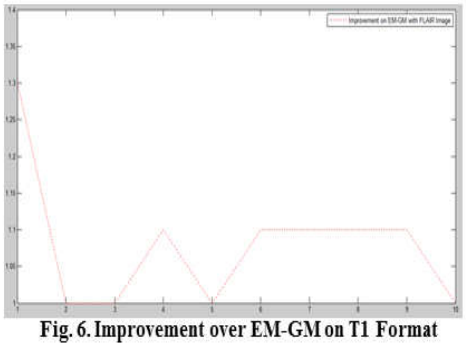

Fig. 6. Improvement over EM-GM on T1 Format

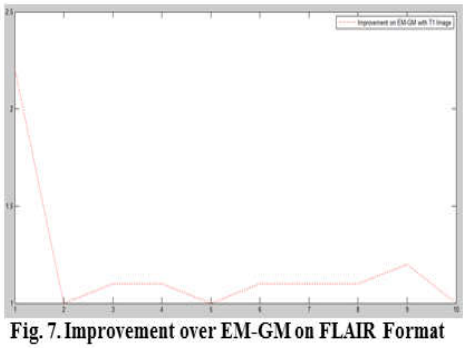

Fig. 7. Improvement over EM-GM on FLAIR Format

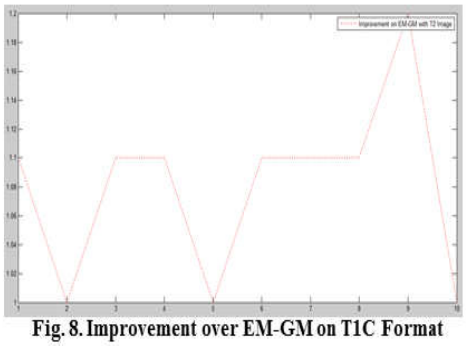

Fig. 8. Improvement over EM-GM on T1C Format

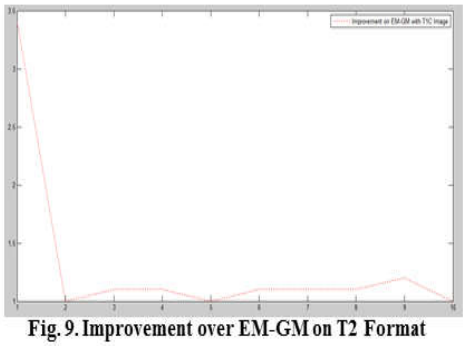

Fig. 9. Improvement over EM-GM on T2 Format

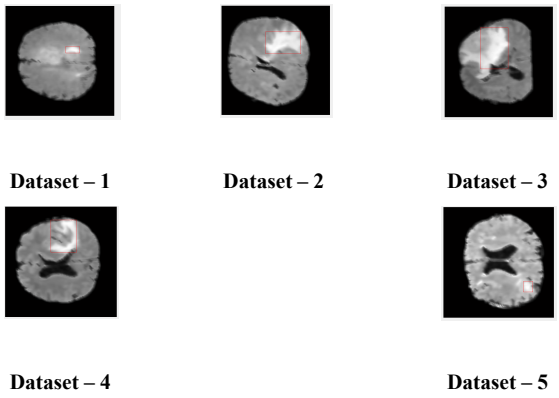

Fig. 10. Disease Prediction for Various Datasets

Conclusion

Major Contributions of this work are the multilateral filter to normalize the image noises and the enhancement of EM-GM technique to improve the detection of brain diseases. Quantitative analysis of brain MR images allows a greater understanding of the nature of the diseases. The proposed algorithm in this work has been tested on BRATS 2012 (Nice), BRATS 2013 (Nagoya) and BRATS 2014 (Boston) challenge datasets and demonstrates higher accuracy. The work also concludes the optimal technique for medical image segmentation and detection of brain anomalies. Compared to the existing research outcomes, this work demonstrates the mapping of possible disease with the brain anomalous regions. With the final outcome of accuracy improvement for FLAIR, T1, T2 and T1C image data types on disease prediction, the work certainly and satisfyingly extends the possibilities of better medical image processing.

REFERENCES

Achanta R. *et al*., "SLICsuperpixels compared to state-of-the-art su- perpixel methods," IEEE Trans. Pattern Anal. Mach. Intell., vol. 34, no. 11, pp. 2274–2282, Nov. 2012

Ahmed, S., K. M. Iftekharuddin and A. Vossough, 2015."Efficacy of texture, shape, and intensity feature fusion for posterior-fossa tumor segmentation in MRI", IEEE Trans. *Inf. Technol. Biomed*., vol. 15, no. 2, pp. 206-213.

Avants B. B. *et al*., "A reproducible evaluation of ANTs similarity metric performance in brain image registration," *Neuroimage*, vol. 54, no. 3, pp. 2033–44, Feb. 2011

Bauer, S., R. Wiest, L.-P. Nolte and M. Reyes, "A survey of MRI-based medical image analysis for brain tumor studies", *Phys. Med. Biol*., vol. 58, no. 13, pp. R97-R129, 2013

Gooya, A., G. Biros and C. Davatzikos, "Deformable registration of glioma images using EM algorithm and diffusion reaction modeling", *IEEE Trans. Med. Imag*., vol. 30, no. 2, pp. 375-390, 2011

Hameeteman, K. 2011. "Evaluation framework for carotid bifurcation lumen segmentation and stenosis grading", *Med. Image Anal*., vol. 15, no. 4, pp. 477-488.

Islam, A., S. M. S. Reza, and K. M. Iftekharuddin, "Multi-fractal texture estimation for detection and segmentation of brain tumors," *IEEE Trans. Biomed. Eng*., vol. 60, no. 11, pp. 3204–3215, Nov. 2013.

Menze B. M. *et al*. "The multimodal brain tumor image segmentation benchmark (BRATS)," *IEEE Trans. Med. Imag*., vol. 33, no. 10, pp. 1993–2024, Oct. 2014.

Shattuck, D. W., G. Prasad, M. Mirza, K. L. Narr and A. W. Toga, "Online resource for validation of brain segmentation methods", *Neuroimage*, vol. 45, no. 2, pp. 431-439, 2009

Shin, H. C., M. R. Orton, D. J. Collins, S. J. Doran, and M. O. Leach, "Stacked autoencoders for unsupervised feature learning and multiple organ detection in a pilot study using 4D Dataset data," *IEEE Trans. Pattern Anal. Mach. Intell*., vol. 35, no. 8, pp. 1930–1943, Aug. 2013

Stille, M.,M. Kleine; J. Hagele; J. Barkhausen; T. M. Buzug, "Augmented Likelihood Image Reconstruction", IEEE Transactions on Medical Imaging, Volume:35, Issue:1

Subbanna, N., D. Precup, L. Collins, and T. Arbel, "Hierarchical prob- abilistic Gabor and MRF segmentation of brain tumours in MRI vol- umes," *Proc. MICCAI*, vol. 8149, pp. 751–758, 2013

Weizman, L. 2012. "Automatic segmentation, internal classification, and follow-up of optic pathway gliomas in MRI", *Med. Image Anal*., vol. 16, no. 1, pp. 177-188.

****